

Received November 5, 2020, accepted December 4, 2020, date of publication December 14, 2020, date of current version December 31, 2020.

Digital Object Identifier 10.1109/ACCESS.2020.3044249

# Study on Energized Mixed-phase Icing of CFCCW and Its Effect on AC Corona Onset Voltage

BINGBING DONG<sup>1,2</sup>, (Member, IEEE), JIALE SONG<sup>1</sup>, CHANGSHENG GAO<sup>1</sup>, ZELIN ZHANG<sup>1</sup>, YU GU<sup>1</sup>, AND NIANWEN XIANG<sup>1</sup>, (Member, IEEE)

<sup>1</sup>School of Electrical Engineering and Automation, Hefei University of Technology, Hefei 230009, China

<sup>2</sup>Far East Holding Group Company, Ltd., Yixing 214257, China

Corresponding author: Bingbing Dong (bndong@hfut.edu.cn)

This work was supported in part by the Science and Technology Project of State Grid Corporation under Grant W2020JSKF0677, in part by the Joint Fund of National Natural Science Foundation of China under Grant U1834204, and in part by the 111 Project under Grant BP0719039.

**ABSTRACT** In winters, China witnesses frequent mixed-phase ice disasters, which have a detrimental impact on the secure operation of transmission lines. Most of the studies are focused on the conventional overhead lines, and little attention is paid to the novel carbon fiber composite core wire (CFCCW), which were widely used in recent years. Besides, the influence rule of frequent mixed-phase icing on the corona onset characteristics for CFCCW has not been extensively studied across extant literature. Thus, this article addresses the aforementioned issues by conducting Alternating Current (AC) corona tests for four kinds of CFCCW that would be coated by mixed-phase ice in a low-temperature laboratory. The results showed that the impact of mixed-phase ice on the wire corona onset voltage can be reduced by nearly 50%. With more icing the corona onset voltage would further decrease but at a slower pace. For the wires with a larger diameter, higher corona onset voltage with low distortion in the electric field strength was observed for the same icing time. For the freezing-water conductivity, no significant impact on both the icing morphology and the corona onset voltage was observed. Moreover, the validation for the simulation model was established by comparing the simulation results with the experimental results. These inferences drawn could act as a theoretical reference for transmission lines designing and calculating the wire corona onset voltage in the mixed-phase icing areas.

**INDEX TERMS** CFCCW, energized icing, mixed-phase, ac corona onset voltage.

## I. INTRODUCTION

Compared with conventional LGJ series aluminum conductor steel reinforced, the novel CFCCW possess lighter weight, higher strength, better corrosion resistance, and larger capacity, which facilitates its wide-ranging applications in transmission lines [1]–[4]. The development of UHV and long-distance transmission technologies had necessitated the development of the transmission lines that can withstand extremely harsh physical conditions. In the winter of China, freezing rain and heavy fog can easily cause mixed-phase icing, which leads to the formation of iced transmission lines and causes serious power outages [5]–[7]. The first two months of 2008 alone had witnessed the occurrence of massive snow and ice disasters, and their detrimental impact

on the electric power facilities in China. Since then, there had been a surge in extensive research on the corona onset characteristics for iced overhead conductors in China and elsewhere [8], [9]. The existing studies have confirmed that icing can cause a change in the surface roughness of the conductors and thereby induce serious distortion in its surface electric field, leading to an impact on the corona onset voltage [5]. However, currently, there are only sporadic and limited investigations on the corona onset characteristics for iced CFCCW.

A few studies have investigated the characteristics of conductor corona onset under various external environmental conditions, including clean, dirty, rainy, high altitude and icy [10]–[19]. In the earlier study, the empirical formula of the corona onset field strength of conductors was obtained by summarizing a large number of experiments [20]. However, the classic Peek's law used for calculating the corona

The associate editor coordinating the review of this manuscript and approving it for publication was Sofana Reka S<sup>1</sup>.

onset voltage does not consider the impact of the external environment, such as icy conditions. Therefore, in practical situations, the results obtained of corona onset voltage varied drastically from laboratory value. As the mixed-phase icing is an alternating combination of the two layers of glaze and grime that grows rapidly and causes severe damage to the conductor [10]–[12]. It was implied that the formation of the mixed-phase icing can alter the electric field distribution on the surface of the conductor. The formation of branch-shaped ice and icicles causes distortions in the electric field of the conductor. Under such circumstances, corona discharge can occur even at comparatively lower voltages, which makes the lowering of the corona onset voltage imperative for the conductor [13]–[15].

In practical applications, the conductor is covered by both glaze ice and rime ice and these icing morphologies impact the corona onset voltage under the frequent mixed-phase icing conditions. The influence of the alternating current (AC) electric field on the icing morphology was investigated, and the corona discharges, under different rime branch formations, were measured [21]. This study inferred that the variation in rime morphology can also affect the corona discharge in the case of longer and shaper branch-shaped ice, the conductor corona discharge occurs at a lower voltage. The previous studies have established the significance of knowledge about conductor corona discharges under clean, rainy, dirty or iced conditions [21]–[23]. Accompanying with the widespread use of CFCCW, the complex geographical icy terrains of China have made it necessary to conduct an in-depth analysis of the corona onset performance under the icing conditions to overcome the detrimental impact of corona discharges. As a novelty, CFCCW have rarely been compared with the ordinary stranded wires for performance in the icy external environment. Ref. [24], while comparing the performances of CFCCW with other standard wires firstly observed that both types of wires demonstrated a nonlinear increase in icing thickness and icicle length over time. Secondly, the study observed that for the same diameter, CFCCW demonstrated a faster growth in icing thickness but a slower increase in icicle length as compared to others. Lastly, the study observed that faster ice thickening and icicle length growth associates with the decrease in diameter.

Therefore, to investigate the influence rule of the electric field during mixed-phase icing on the corona onset voltage of conductors, this article employs an ultraviolet (UV) imager in a low-temperature laboratory for measuring the corona onset voltage of CFCCW. The wires, used in testing, were JRLX/T-150/28, JRLX/T-240/28, JRLX/T-310/40, JRLX/T-517/71 and the I-U curve fitting method is adopted to analyze the variation mechanism of the corona onset voltage. Correspondingly, the impact of conductivity and icing level on corona onset voltage was studied. Based on the mixed-phase icing morphology and the gas discharge theory, a finite element model of corona onset discharge was established to calculate the electric field and to obtain the electric field variation trends on the surface CFCCW. These results can

provide a point of reference for the design and selection of the transmission lines in mixed-phase ice-prone locations.

## II. TEST EQUIPMENT, SPECIMENS AND PROCEDURE

### A. EXPERIMENTAL EQUIPMENT

The test is implemented in the cryogenic climate chamber with an internal diameter of 2 m and internal length of 4 m. The temperature can drop to as low as  $-30\text{ }^{\circ}\text{C}$  and standard spray nozzles recommended by IEC are installed in the chamber. Therefore, different icing forms can be simulated, such as glaze, soft rime and hard rime. The fan in the chamber not only imitates wind at a certain speed but also evenly distributes indoor temperature and particle size. The test voltage is introduced from one side of the chamber by porcelain casing, and the diagram of the test principle is shown in Fig. 1. Note, T: voltage regulator, 10 kV. B: AC testing transformer, ratio is 1:15.  $R_0$ : protective resistance, 100 k $\Omega$ . H: high voltage wall bushing, 110 kV. F: AC capacitor divider (ratio 10000:1).  $C_1$  and  $C_2$ : high and low voltage capacitors, 4  $\mu\text{F}$  and 400 pF. V: voltmeter, P: artificial climate chamber, S: conductor, N: corona cage, K: insulator, L: grading ring, Ca: UV imaging instrument.

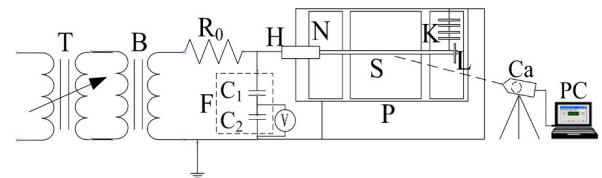


FIGURE 1. Schematic diagram of AC test circuit.

### B. SPECIMENS

The CFCCW undergo energized mixed-phase icing in the center of a three-section corona cage with a diameter of 2 m and length of 2.5 m, and the middle section is specifically designed to measure COV and others grounded. The wires, used in testing, were JRLX/T-150/28, JRLX/T-240/28, JRLX/T-310/40, JRLX/T-517/71 with lengths of 2.0 m are used. The ends of the wires are fitted with grading rings to eliminate the ending effect. The structural parameters are shown in Table I,  $D_t$  represents the diameter of carbon fiber core;  $D_w$  represents the wire diameter;  $n$  represents the number of strands of conductors;  $L_w$  is the length of a single wire. The mixed glaze is formed by the alternate icing of first glaze and then rime, and the alternate time is the same. The forming condition of the mixed-phase Icing in the chamber is shown in Table II, where  $d_a$  is the droplet diameter,  $W$  is the absolute humidity,  $T_a$  is the formation temperature of the glaze in this test (not a fixed value),  $\gamma_{20}$  is the water conductivity in  $20\text{ }^{\circ}\text{C}$  used to simulate glaze. To, PTU200 which is a digital temperature, humidity and pressure device is used to gauge environmental parameters. Droplet diameter and absolute humidity are measured by a laser particle analyzer. The conductivity is measured by a DD-810E meter. As the major extent of the spectra produced by the corona discharge

**TABLE 1. Technical Parameters and Numbers of Four CFCCW.**

Type	Specimens	$D_f$ /mm	$D_w$ /mm	$n$	$L_w$ /m
#1	JRLX/T-150/28	6.0	15.6	15	2
#2	JRLX/T-240/28	6.0	19.0	16	2
#3	JRLX/T-310/40	7.1	23.0	16	2
#4	JRLX/T-517/71	9.5	28.1	22	2

**TABLE 2. Forming Conduction for Mixed-Phase Ice.**

Type	$d_i$ ( $\mu$ m)	W(g/cm <sup>3</sup> )	$T_a$ ( $^{\circ}$ C)	$\gamma_{20}$ ( $\mu$ S/cm)
Glaze	100	8.5	-5	30 400 800 1200
Rime	20	2.5	-15	30 400 800 1200

is in the invisible UV region, CoroCAM IV+ UV imager is used to observe the development of corona discharge because an obvious relationship exists between photon numbers and COV.

**C. CRITERION FOR CORONA ONSET VOLTAGE**

We always place the UV camera outside the chamber, fix the distance between the conductor and the camera, and directly measure the wires by using the camera through a big window without glass to measure the COV values after icing. By applying 90% of the predicted COV to the iced wire, the boosting speed of the voltage is maintained at 3 kV/s until the photons are observed through the camera. Therefore, a 30 s video was taken to record the change in photon quantity after a 1 min interval under the voltage [23], [24]. Fig. 2 shows the photon pictures of JRLX/T-240/28 after icing for 30 min at 15 kV/cm captured by the UV camera. Only a few photons appear when the voltage is  $\leq 30.1$  kV, Fig. 2(a), show that

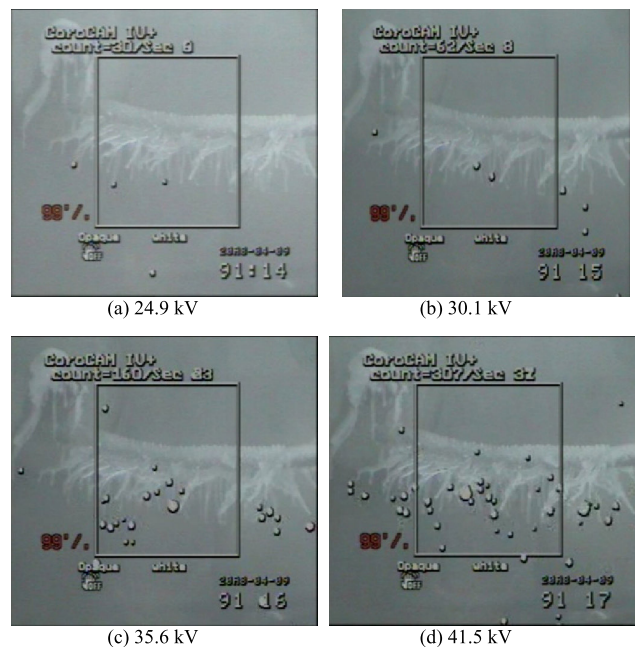


**FIGURE 2. Corona discharge images of JRLX/T-240/28 after mixed phase icing.**

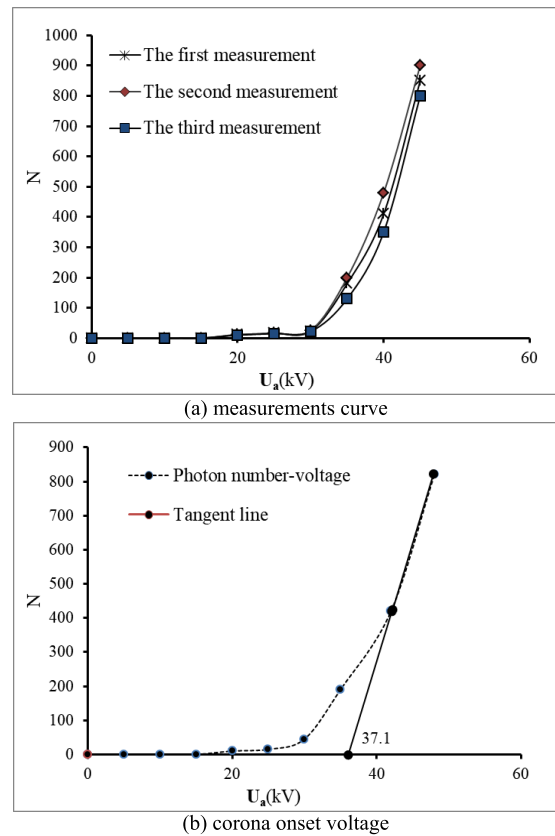


**FIGURE 3. Calculation for conductor corona onset voltage.**

corona discharge does not occur. When the voltage is set to a value  $\geq 35.6$  kV, the camera captures a sudden increase in the number of photons, Fig. 2(b) to 2(a).

Therefore, we deduced that the COV should be around 35.2-41.5 kV. The average photon number is calculated from the 30 s video and measured three times. The photon-voltage curves are shown in Fig. 3(a), where  $N$  is the number of photons, and  $U_a$  is the test voltage. The deviation is acceptable because each couple of three tests is  $\leq 7.5\%$ . The voltage corresponding to the knee point of the photon-voltage curve is the COV value, as shown in Fig. 3(b).

**III. TEST RESULTS AND ANALYSES OF CORONA ONSET VOLTAGES**

**A. MORPHOLOGY OF MIXED-PHASE ICE**

To investigate the influence of the electric field strength, during the mixed-phase icing, on the corona onset voltage of CFCCW, the conductivity of the freezing-water was fixed at 400  $\mu$ S/cm (calibrated to 20  $^{\circ}$ C), the icing time was fixed at 30 minutes, and the electric field strength was kept at 0~20 kV/cm. The morphology of the mixed-phase ice on CFCCW caused the electric field strength variations, which resulted in a relatively large difference in the corona onset voltage. The mixed-phase ice morphology and corona onset voltage of CFCCW under different electric field strengths during icing are depicted in Fig. 4. The corona onset voltage of CFCCW

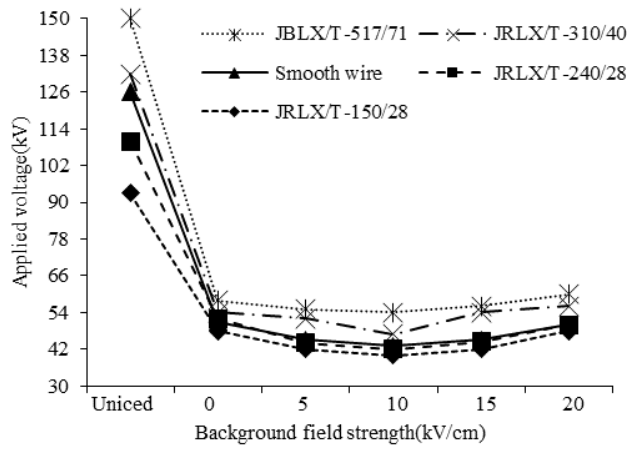


FIGURE 4. Corona onset voltage under different icing field.

reflected the variation in the electric field strength during the mixed-phase icing. Consequently, the corona onset voltage after icing was reduced dramatically. Even at the electric field strength of 20 kV/cm, with the shortest icicle and the bluntest ice tip, the residual corona onset voltage was only around 50% of the original value. The main cause behind it is that the increase in the mixed-phase ice, there is an increase in the surface roughness of the wire, causing changes in its original form. This causes the electric field on the wire surface distortion and shows corona discharge even at rather lower voltages.

As depicted in Fig. 4, with the increase in the electric field strength during icing, the corona onset voltage first decreased and then increased. For the electric field strength of 0-10 kV/cm during icing, due to the electric field attraction, the mixed-phase icicles grew rapidly. Besides, with higher electric field strengths, the water drops stretched more along the direction of the electric field. Therefore, the drop diameter of the water drops that could stably exist at the tips become smaller and leads to the manifesting of thinner ice tips. This caused more significant electric field distortions at the icicle tip and further reduced the corona onset voltage. With the application of electric field strength of 15-20kV/cm on the iced wire, the Coulomb impulse noted in the water drop was positive. The electric field then exerts a repelling force on the water drop, shortening the icicle length. Meanwhile, intensifying ion bombardment and corona discharge activities accelerate the melting and blunting of the tip of the icicles, leading to the formation of branch-like ice. Therefore, it can be inferred that by raising the corona onset voltage, the distortion of the surface electric field, induced by the mixed-phase ice, can be diminished.

**B. INFLUENCE OF MIXED-PHASE ICING LEVEL ON WIRE CORONA ONSET VOLTAGE**

The morphology of the mixed-phase ice changes with the icing time increases gradually. To investigate the influence

TABLE 3. Coefficient of JRLX/T-517/71 Conductor in 15~60min Mixed-Phase Icing Under 5~20 kV/cm.

	$E_a$ (kV/cm)				$T$ (min)			
	5	10	15	20	15	30	45	60
$K$ (mm)	4.91	5.62	2.81	1.94	2.05	3.34	4.53	5.21
$O$ (mm)	1.53	1.53	1.55	1.52	1.56	1.55	1.53	1.55
$P$ (mm)	1.54	1.59	1.46	1.33	1.43	1.45	1.44	1.45
$L$ (cm)	2.74	3.01	2.13	1.53	0.61	1.31	1.95	2.45
$M$ (mm)	6.2	6.5	7.1	8.2	5.2	5.8	6.7	8.3
$N$ (mm)	4.3	3.4	4.7	5.8	4.8	4.7	4.4	4.2

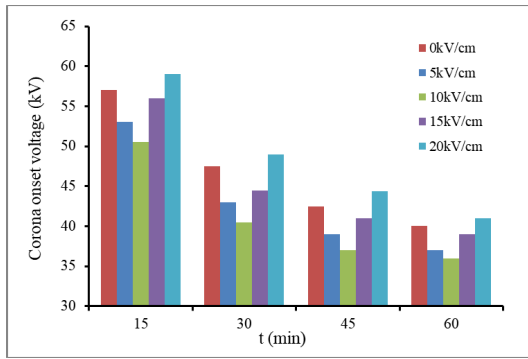
of the icing level on the corona onset voltage of CFCCW, the icing time kept at 15~60 minutes. The experimental results obtained are shown in Fig. 5.

As shown in Fig. 5, for different electric fields, with the icing time increases gradually, the corona onset voltage decreases gradually. It implies that the increased icing time led to so ice coating that more significant distortions in the surface electric field. On the other hand, at the glaze icing stage, the thickened ice reduces the collision efficiency of the water drops. Consequently, a longer time is required for the drops to flow to the ice tip, which mitigates the distortion effect about the icicles. The icing time has no influence on the morphology parameters of the branch-shaped rime ice. Besides, this phenomenon enhanced the effective diameter of the wire while further reducing the collision efficiency. Ultimately, due to the growth of the mixed-phase ice, a relatively long time was required for the wire corona onset voltage drop and eventual saturation.

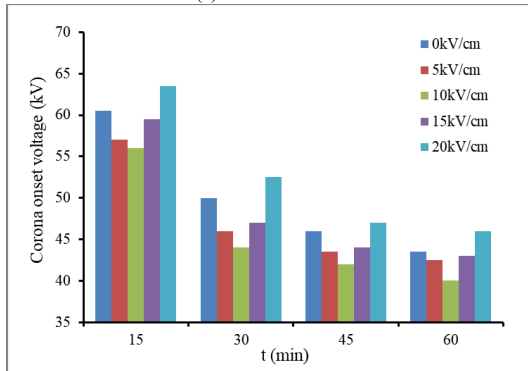
**C. INFLUENCE OF FREEZING-WATER CONDUCTIVITY ON CORONA ONSET VOLTAGE**

The transmission line’s surface has high conductivity, which affects the corona onset voltage characteristics. To investigate this effect during the experiment, the conductivity of the freezing water was configured to be 30~1200  $\mu$ S/cm at a temperature of 20°C. The coating time of mixed-phase ice was kept at 30 minutes in all four conductivity cases, and the electric field was varied. The close-up morphology of the mixed-phase ice and the corona onset voltages are shown in Fig.6. It can be observed that when the electric field strength was 15 kV/cm during icing, the conductivity variation had little effect on the morphology of the mixed-phase ice. Correspondingly, the corona onset voltages remained the same and did not change regularly as a function of the conductivity. Thus, it was inferred that the conductivity has no influence on corona onset voltage. This was because the mixed-phase ice was coated alternatively by dry and wet ice. So, the freezing-water conductivity had little effect on the corona discharge of the surface rime. Besides, the glaze icicles at the lower wire surface had no water films, due to the low external temperature, which could be regard as dry ice. Moreover, the icing morphology depicted similar even with different salinities. These factors contributed to an almost unvaried corona onset voltage for the wire.

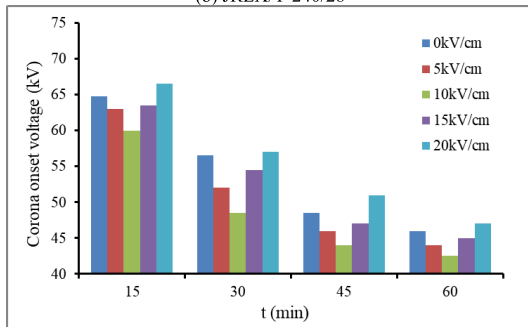




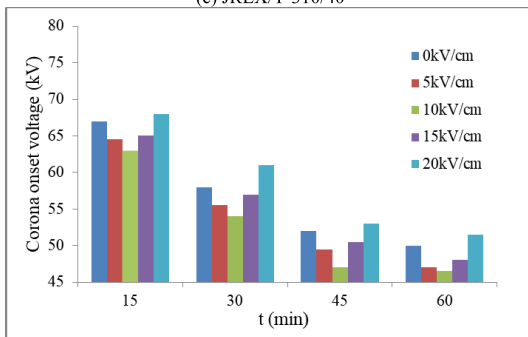
(a) JRLX/T-150/28



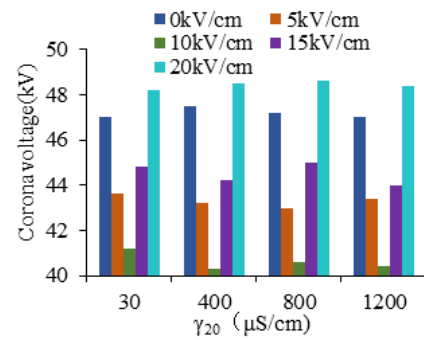
(b) JRLX/T-240/28



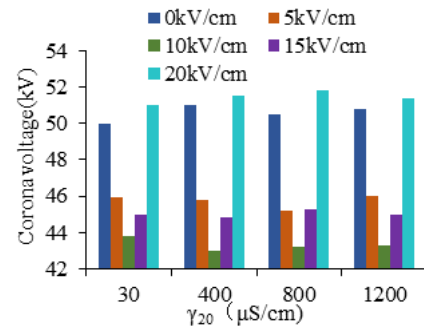
(c) JRLX/T-310/40



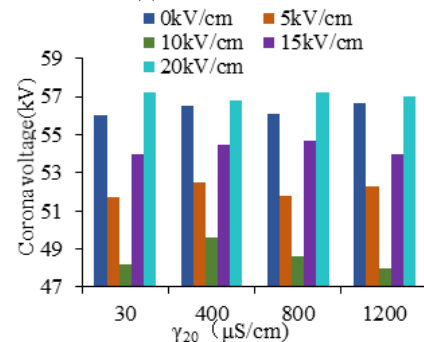
(d) JRLX/T-517/71



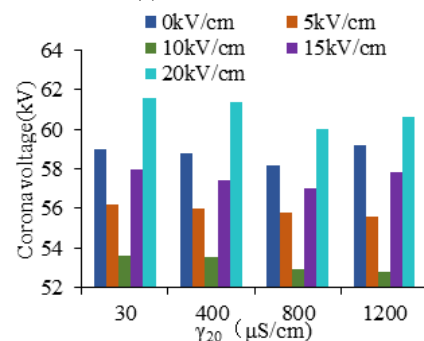
(a) JRLX/T-150/28



(b) JRLX/T-240/28



(c) JRLX/T-310/40



(d) JRLX/T-517/71

FIGURE 5. Relationship between corona onset voltage and icing time.

#### IV. INFLUENCE OF MIXED-PHASE ICE ON SURFACE FIELD STRENGTH

##### A. FINITE ELEMENT CALCULATION SETTING

The finite element model is established by using Maxwell software. Considering the iced conductor of the 2.0 m diameter coaxial electrode, the conductor's material is set

FIGURE 6. Corona onset voltage under different conductivity.

to Aluminum and relative permittivity of glaze is 75, the background region is set to vacuum while boundary of the corona cage is set to the balloon border condition with an infinity potential of zero, after that, an automatic mesh is generated and calculated. The glaze parameters of

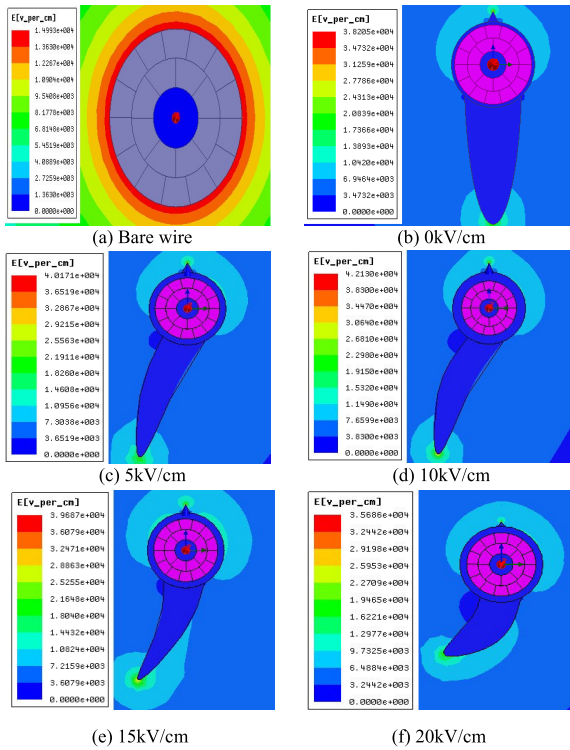


FIGURE 7. Field distribution of mixed-phase icing under different field.

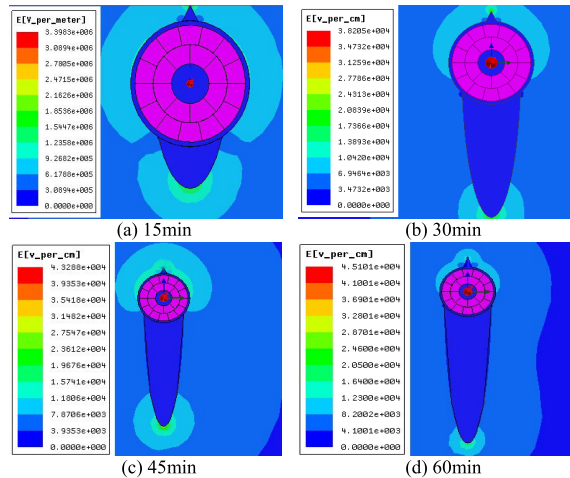


FIGURE 8. Field distribution on the surface of JRLX/T-517/71 under 0kV/cm mixed-phase icing.

JRLX/T-517/71 under 5~20kV/cm and 15~60min are shown in Table III, where  $E_a$  is the icing field,  $K$  is the ice thickness,  $L$  is the length of icicle,  $O$  and  $P$  are the bottom diameters and height of the ice branches respectively,  $M$  and  $N$  are the top and tip diameters of the icicle respectively, and  $T$  is the icing time.

**B. ANALYSIS OF RESULTS FROM DIFFERENT ELECTRIC FIELD STRENGTHS**

From Fig. 7(a), the surface electric field strength of the JRLX/T-517/71 CFCCW with no icing was 15 kV/cm, under the 90 kV AC. For the electric field of 0-20 kV/cm, the surface

of iced wire electric field strength at 38.2, 40.2, 42.1, 39.7, and 35.7kV/cm sequentially, showing a trend of increase at first and decrease afterward as shown in Fig. 7(b)-(f). The reason is that from 0-10 kV/cm the icicles became longer and thinner with the increase in electric field strength and causes serious distortions in the electric field of the wire surface. However, from 15-20 kV/cm, a gradual reduction in the maximum surface electric field strength is observed due to the icicles shortened and thickened.

**C. ANALYSIS OF RESULTS FROM DIFFERENT MIXED-PHASE ICING LEVELS**

As shown in Fig. 8, when CFCCW was iced for a varying time from 15-60 minutes, the surface electric field strength was 34.0, 38.2, 43.3, and 45.1kV/cm, respectively, showing a gradual upward tendency under the same operating voltage of 90kV. This was due to the diminishing of both the growth of mixed-phase icicles and the speed of the ice tip diameter, with an increase in the icing time. Therefore, the increase of the surface electric field also lowered gradually, consistent with the trend in the experiment.

**V. CONCLUSION**

(1) The mixed-phase icing can cause the corona onset voltage of CFCCW to decrease. At the early stages of icing, there was an approximately 50% reduction in the corona onset voltage noted. CFCCW with larger diameter showed higher corona onset voltage. Further, the corona onset voltage of CFCCW was observed to be higher than that of a traditional conductor with the same diameter. For a set icing time, with the increase in the electric field strength during icing, the corona onset voltage of CFCCW decreased at first and then increased.

(2) Under the mixed-phase icing condition, with the increasing level of icing, the corona onset voltage of CFCCW dropped constantly. However, the speed of corona onset voltage dropped gradually slowed and eventually saturated. The conductivity variation of the freezing water did not manifest an obvious change in the mixed-phase ice morphology of CFCCW, and the corresponding variation in the corona onset voltage was negligible.

(3) The mixed-phase icing can generate serious distortions in the surface electric field strength of the energized wires, causing the corona discharge at low voltages. Due to the increase in the surface electric field strength during icing, the surface electric field of the iced CFCCW increases at first and then decreases. With an increase in icing time, the surface electric field continues to intensify gradually. The maximum surface electric field strength demonstrated a regular change when the electric field during icing or even the level of the icing was varied. This was consistent with the variation law of the corona onset voltage obtained during the experiments, which validated the established model.

**ACKNOWLEDGMENT**

The authors would like to thank the contributions of Prof. Xingliang Jiang for his work on the test plan and writing guide

of this document. The authors acknowledge the contributions of Engineer Man Zhang for his work on the test implementation. The authors also would like to thank all members of the external insulation research team at Chongqing University for their contributions to this article.

## REFERENCES

- [1] B. Liu, P. Dang, and S. Z. Ji, "Development and application of hollow wire with concentric gallow," (in Chinese), *Electr. Wire&Cable*, no. 6, pp. 9–12, Dec. 2008.
- [2] H. Jin, S. Nie, C. Tong, Z. Li, S. Wei, and N. Gao, "Investigation on anti-icing mechanism of super-hydrophobic aluminum wire," *Proc. CSEE*, vol. 37, no. 4, pp. 204–230, 2010.
- [3] D. P. Zhu, B. Ouyang, and J. H. Wang, "Discussion on the development and application of concentric gallow hollow conductor for ice and snow resistance," (in Chinese), in *Proc. 10th Annu. Conf. China Assoc. Sci. Technol. Innov. Ind. Strong City Strategy Forum*, Sep. 2008, pp. 52–58.
- [4] J. H. Jiang, "Comparison of main properties between steel-cored aluminum strand and steel-cored aluminum strand," (in Chinese), *Electr. Wire Cable*, no. 1, pp. 19–22, Feb. 2012.
- [5] M. Zhang, X. L. Jiang, L. C. Shu, J. L. Hu, J. Chen, and Y. J. Guo, "Influence of mixed-phase on high voltage of split wires," *J. Electrotechnics*, vol. 30, no. 3, pp. 258–267, 2015.
- [6] X. Jiang, Z. Zhang, Q. Hu, J. Hu, and L. Shu, "Thinkings on the restrike of ice and snow disaster to the power grid," *High Voltage Eng.*, vol. 44, no. 2, pp. 463–469, 2018.
- [7] C. L. Bi, X. L. Jiang, X. B. Han, Z. Y. Yang, and X. D. Ren, "Anti-icing method of using expanded diameter conductor to replace bundle conductor," *Trans. China Electrotech. Soc.*, vol. 35, no. 11, pp. 2469–2477, 2020.
- [8] X. Y. Zeng, J. W. Liu, and Y. Huang, "Analysis on the significance of UHV AC transmission," (in Chinese), *Eng. Technol. Ind. Economy*, vol. 8, no. 2, pp. 21–22, 2009.
- [9] X. L. Jiang, F. Y. Jiang, Q. L. Wang, B. Luo, and X. Han, "Prediction of rime accretion on transmission line based on optimal time step model," (in Chinese), *Trans. China Electrotech. Soc.*, vol. 33, no. 18, pp. 4408–4418, 2018.
- [10] Z. Y. Li, X. L. Jiang, L. C. Li, Q. Hu, and L. C. Shu, "Corona performance of coated conductors under raining condition," (in Chinese), *High Voltage Eng.*, vol. 43, no. 11, pp. 3740–3747, 2017.
- [11] Y. Hu, J. X. Hu, and T. Liu, "Analysis and countermeasures for large area icing accident on power grid in northern China," *Electr. Equip.*, vol. 9, no. 6, pp. 1–4, 2008.
- [12] F. C. Lü, S. H. You, Y. P. Liu, and Q. F. Wan, "Analysis on corona loss measurement of ultra-high voltage AC single circuit test line in rain and snow weather conditions," (in Chinese), *High Voltage Eng.*, vol. 37, no. 9, pp. 2089–2095, 2011.
- [13] I. Ndiaye, I. Fofana, and M. Farzaneh, "Contribution to the study of the appearance and development of corona discharges on a surface of ice," in *Proc. Canadian Conf. Elect. Comput. Eng. Caring Humane Technol.*, vol. 1, May 2003, pp. 639–642.
- [14] D. B. Phillips, R. G. Olsen, and P. D. Pedrow, "Corona onset as a design optimization criterion for high voltage hardware," *IEEE Trans. Dielectr. Electr. Insul.*, vol. 7, no. 6, pp. 751–774, Dec. 2000.
- [15] Y. Liu and B. Du, "Recurrent plot analysis of leakage current on flashover performance of rime-iced composite insulator," *IEEE Trans. Dielectr. Electr. Insul.*, vol. 17, no. 2, pp. 465–472, Apr. 2010.
- [16] Y. W. Xue, L. Yang, Y. P. Hao, Y. Gu, and L. Li, "A comparative study on icing morphology and process of glaze and light rime in suspension composite insulators on transmission lines," (in Chinese), *Trans. China Electrotech. Soc.*, vol. 31, no. 8, pp. 212–219, 2016.
- [17] Z. X. Li, J. B. Fan, Y. Yin, and G. Chen, "Numerical calculation of the negative onset corona voltage of high-voltage direct current bare overhead transmission conductors," *IET Gener., Transmiss. Distrib.*, vol. 4, no. 9, pp. 1009–1015, 2010.
- [18] X. D. Liang, Y. J. Li, Y. B. Zhang, and Y. T. Liu, "Time-dependent simulation model of ice accretion on transmission line," (in Chinese), *High Voltage Eng.*, vol. 40, no. 2, pp. 336–343, 2014.
- [19] X. M. Bian, L. Chen, D. M. Yu, L. M. Wang, and Z. C. Guan, "Surface roughness effects on the corona discharge intensity of long-term operating conductors," *Appl. Phys. Lett.*, vol. 101, no. 17, pp. 174103–174104, 2012.
- [20] G. Hartmann, "Theoretical evaluation of Peek's law," *IEEE Trans. Ind. Appl.*, vol. 20, no. 6, pp. 1647–1651, Nov. 1984.
- [21] L. C. Shu, T. Li, X. L. Jiang, Q. Hu, B. S. Luo, and Z. G. Yang, "Influences of AC electric field strength on conductor rime icing performance," *Proc. CSEE*, vol. 32, no. 19, pp. 140–147, 2012.
- [22] J. Z. Lu, J. P. Hu, Z. Fang, and Z. L. Jiang, "Icing accretion and ice-melting test at Xiaoshajiang natural disasters test site in Xuefeng Mountain," (in Chinese), *High Voltage Eng.*, vol. 40, no. 2, pp. 388–394, 2014.
- [23] F. H. Yin, X. L. Jiang, and F. Masoud, "Influences of electric field of conductors surface on conductor icing," *High Voltage Eng.*, vol. 44, no. 3, pp. 1023–1033, 2018.
- [24] L. C. Shu, B. S. Luo, Q. Hu, X. L. Jiang, T. Li, and Y. Zhang, "Comparative analysis of rime covering characteristics between tile wire and ordinary stranded wire," *High Voltage Technol.*, vol. 38, no. 6, pp. 1466–1470, 2012.



**BINGBING DONG** (Member, IEEE) was born in Anhui, China, in September 1987. He received the Ph.D. degree in engineering from Chongqing University, China, in 2014. He is currently a Lecturer with the School of Electrical Engineering and Automation, Hefei University of Technology, Hefei, China. He is currently a Postdoctoral Scholar with the Hefei University of Technology and Far East Holding Group Company Ltd. He has published over 30 articles about his professional work. His main research interests include high voltage technology, pulsed-power and plasma technology, external insulation and transmission lines, and the condition monitoring of power apparatus.



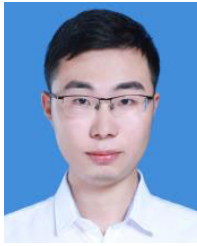
**JIALE SONG** was born in Shandong, China, in 1998. He received the B.S. degree from the Hefei University of Technology, Hefei, China, in 2020, where he is currently pursuing the M.S. degree in electrical engineering. His research interest includes pulsed-power and plasma technology.



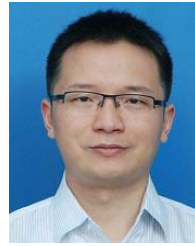
**CHANGSHENG GAO** was born in Anhui, China, in 1998. He received the B.S. degree from the Chongqing University of Technology, in 2020. He is currently pursuing the M.S. degree in electrical engineering from the Hefei University of Technology, Hefei, China. His research interests include pulsed-power and plasma technology.



**ZELIN ZHANG** was born in Shanxi, China, in 1997. He received the B.S. degree from the Hefei University of Technology, Hefei, China, in 2019, where he is currently pursuing the M.S. degree in electrical engineering. His research interest includes transmission line icing and protection.



**YU GU** was born in Anhui Province, China in 1996. He received the B.S. degree from the Anhui Jianzhu University in 2018. He is currently pursuing the M.S. degrees in electrical engineering from the Hefei University of Technology, Hefei, China. His research interests include condition monitoring of power apparatus.



**NIANWEN XIANG** (Member, IEEE) was born in China in 1985. He received the Ph.D. degree in electrical engineering from North China Electric Power University, Beijing, in 2017. In 2017, he joined Hefei University of Technology, Hefei, China. His current research interests include electromagnetic compatibility and lightning protection technology for power systems and railway systems, electrical insulation and materials, and the condition monitoring of power apparatus.

...